

Application News

AGX™-V2 AUTOGRAPH Precision Universal Testing Machine
HITS™-TX High Speed Tensile Testing Machine DUH™-210 Dynamic Ultra Micro Hardness Tester
DSC-60 Plus Differential Scanning Calorimeter SPM-Nanoa™ Scanning Probe Microscope
AIRsight™ Infrared and Raman Microscope

Multifaceted Evaluation of Changes in Physical Properties of Recycled Plastics by Advanced Recycling Process and Influencing Microstructural Changes (Part 1): Example of Application to Container/Packaging-Derived Recycled Polyethylene

Yuki Nishikawa¹, Mana Oshiro¹, Mitsuru Ohta¹, Eiji Iida¹, Shoko Iwasaki¹, Zen Miyazaki¹, Takahiko Makise², Shigeru Yao³
1 Shimadzu Corporation, 2 Toyama Kankyo Seibi, 3 Fukuoka University

User Benefits

- ◆ Evaluation of changes in the microscopic physical structures in plastic during molding is possible by multifaceted measurements using general-purpose instruments.
- ◆ It is possible to understand the physical properties of plastics and the factors that influence those properties.

■ Introduction

In response to heightened awareness of decarbonization and a recycling society in recent years, initiatives for plastic recycling are advancing worldwide. However, multiple issues have been pointed out in product applications of recycled plastics, including deterioration of mechanical properties and thermal properties, odor, estimation of life, variations in product quality, and the cost balance. Among those problems, deterioration of mechanical properties is recognized as a problem that requires improvement in many industries because it is directly related to the safety and stable quality of products. The causes of deterioration of mechanical properties are considered to be degradation of the used plastic and the effects of foreign substances. Conventionally, the effect of chemical changes was believed to be the major factor in degradation, but more recently, the results of research at Fukuoka University¹⁾ have revealed that not only chemical changes, but also physical changes have a large effect. One principal cause of this physical changes is considered to be changes in the microscopic physical structures in plastics. A molding technology for physical property improvement of the plastic by an advanced recycling process developed by researchers at Fukuoka University has attracted attention as a technique for controlling these microscopic physical structures. In this report, a multifaceted evaluation was carried out to determine whether the advanced recycling process improved the physical properties of recycled plastic and the factors responsible for that improvement.

■ Test Pieces

The materials used in this experiment were pellets of recycled polyethylene (PE) derived from container and packaging material, which was treated by the advanced recycling process, and untreated pellets of the same PE. Due to various problems such as the shape and sorting accuracy of waste plastic, this material was assumed to contain approximately 20 % polypropylene (PP). Sheets were produced by press-molding the pellets, and were then molded to the sample shapes of ISO 527-2 1B and ASTM D1822 Type L test pieces by die cutting. Table 1 shows the test piece shapes and the types of evaluations conducted.

Table 1 Test Piece shapes and Evaluations Conducted

| Test piece shape | Evaluations conducted |
|-------------------|---|
| ISO 527-2 1B | Tensile test, hardness test, DSC, FTIR, SPM |
| ASTM D1822 TYPE L | High speed tensile test |

(The test pieces used in DSC, FTIR and SPM were cut and processed to the corresponding size and state.)

■ Evaluations

First, to investigate the effects of the advanced recycling process on the physical properties of the samples, strain at break and the elastic modulus were evaluated by a static tensile test, and impact property was evaluated by a high speed tensile test. Next, to consider the factors in changes in the strain at break and impact property, the following evaluations were conducted.

- Dynamic ultra micro hardness tester (DUH): Hardness
- Differential scanning calorimeter (DSC): Crystallization start temperature
- Scanning probe microscope (SPM): Intermediate layer distribution and crystal layer distribution
- Fourier transform infrared spectrophotometer (FTIR): Phase separation of PP in PE

■ Evaluation of Strain at Break and Elastic Modulus by Tensile Test

The tensile test was conducted using an AGX-V2 Autograph precision universal testing machine. A TRViewX non-contact digital video extensometer was used as the extensometer. Fig. 1 shows the appearance of the testing machine, and Fig. 2 shows the appearance during a test. Table 2 shows the instrument configuration and test conditions, Fig. 3 shows the stress-strain curves until break of the test pieces, and Table 3 shows the results of measurements of the strain at break. The strain at break with the advanced recycling process increased in comparison with that without the process.



Fig. 1 AGX™-V2



Fig. 2 Appearance during Test

Table 2 Instrument Configuration and Test Conditions

| | |
|-----------------|---|
| Instrument | : AGX-V2 |
| Load cell | : 500 N |
| Grip | : Pneumatic flat grip |
| Extensometer | : TRViewX 240S |
| Software | : TRAPEZIUM™X-V |
| Test speed | : 1 mm/min (measurement of elastic modulus) |
| | : 50 mm/min (measurement to fracture) |
| Gauge length | : 25 mm |
| Number of tests | : n = 7 |
| Grip distance | : 55 mm |

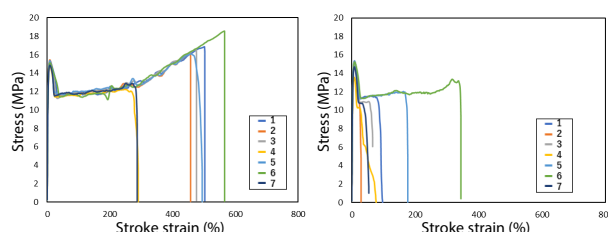


Fig. 3 Stress-Strain Curves to Break
(Left: With Advanced Recycling Process,
Right: Without Advanced Recycling Process)

Table 3 Measurement Results of Strain at Break

| Test piece | Strain at break (%) | Test piece | Strain at break (%) |
|---------------------------------|---------------------|----------------------------------|---------------------|
| W/ Advanced recycling process_1 | 502.7 | W/o Advanced recycling process_1 | 79.73 |
| W/ Advanced recycling process_2 | 457.3 | W/o Advanced recycling process_2 | 29.22 |
| W/ Advanced recycling process_3 | 476.1 | W/o Advanced recycling process_3 | 54.52 |
| W/ Advanced recycling process_4 | 290.2 | W/o Advanced recycling process_4 | 26.64 |
| W/ Advanced recycling process_5 | 494.3 | W/o Advanced recycling process_5 | 176.55 |
| W/ Advanced recycling process_6 | 565.7 | W/o Advanced recycling process_6 | 344.05 |
| W/ Advanced recycling process_7 | 287.0 | W/o Advanced recycling process_7 | 34.44 |
| Average | 439.0 | Average | 106.5 |
| Standard deviation | 108.1 | Standard deviation | 117.1 |
| Coefficient of variation (%) | 25 | Coefficient of variation (%) | 110 |

Fig. 4 shows the stress-strain curves in the elastic region. The black solid line shows the measurement results, and the red line is the approximation line of the elastic modulus calculated in the 0.05 to 0.25 % strain range. Table 4 shows the measured results of the elastic modulus. The elastic modulus with the advanced recycling process is lower than that without the process.

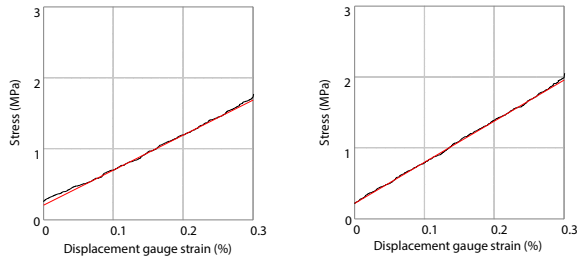


Fig. 4 Stress-Strain Curves of Elastic Region
(Left: With Advanced Recycling Process,
Right: Without Advanced Recycling Process)

Table 4 Measured Results of Elastic Modulus

| Test piece | Elastic modulus (MPa) | Test piece | Elastic modulus (MPa) |
|---------------------------------|-----------------------|----------------------------------|-----------------------|
| W/ Advanced recycling process_1 | 578.3 | W/o Advanced recycling process_1 | 628.2 |
| W/ Advanced recycling process_2 | 549.6 | W/o Advanced recycling process_2 | 579.5 |
| W/ Advanced recycling process_3 | 345.5 | W/o Advanced recycling process_3 | 387.5 |
| W/ Advanced recycling process_4 | 253.8 | W/o Advanced recycling process_4 | 515.9 |
| W/ Advanced recycling process_5 | 457.7 | W/o Advanced recycling process_5 | 636.9 |
| W/ Advanced recycling process_6 | 494.0 | W/o Advanced recycling process_6 | 600.9 |
| W/ Advanced recycling process_7 | 622.4 | W/o Advanced recycling process_7 | 546.0 |
| Average | 471.6 | Average | 556.4 |
| Standard deviation | 131.8 | Standard deviation | 86.0 |
| Coefficient of variation (%) | 28 | Coefficient of variation (%) | 15 |

■ Evaluation of Impact Property by High Speed Tensile Test

The high speed tensile test was conducted using the HITS-TX high speed tensile testing machine. Fig. 5 and Table 5 show the appearance of the instrument and the instrument configuration and the test conditions, respectively. As an example of the test results, Fig. 6 shows the stress-strain curves with and without the advanced recycling process. Tables 6 and 7 show the measured results of the yield stress, strain at break, and break energy in each strain rate with and without the advanced recycling process, respectively. As in the case of the static properties, in comparison with the results without the advanced recycling process, the results of the high speed tensile test with the process showed an increase in strain at break, and break energy also increased.

Table 5 Instrument Configuration and Test Conditions

| | |
|-----------------|---|
| Instrument | : HITS-TX |
| Load cell | : 2 kN |
| Grip | : Flat grip for high speed tensile test |
| Extensometer | : Chuck displacement gauge |
| Software | : TRAPEZIUM HITS |
| Test speed | : 100, 10, 1/s |
| Number of tests | : n = 5 |
| Grip distance | : 40 mm |



Fig. 5 HITS™-TX

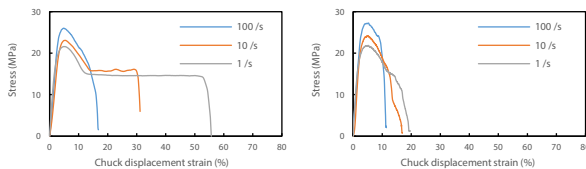


Fig. 6 Stress-Strain Curves
(Left: With Advanced Recycling Process,
Right: Without Advanced Recycling Process)

Table 6 Measured Results of Strain at Break with Advanced Recycling Process
(Average of N = 5)

| Strain rate (/s) | Yield stress (MPa) | Strain at break (%) | Break energy (J) |
|------------------------------|--------------------|---------------------|------------------|
| Average | 26.6 | 18.5 | 0.349 |
| Standard deviation | 0.729 | 5.01 | 0.106 |
| Coefficient of variation (%) | 2.74 | 27.1 | 30.5 |
| Average | 23.0 | 30.7 | 0.492 |
| Standard deviation | 0.290 | 6.70 | 0.131 |
| Coefficient of variation (%) | 1.26 | 21.8 | 26.6 |
| Average | 20.9 | 51.3 | 1.03 |
| Standard deviation | 0.475 | 15.8 | 0.524 |
| Coefficient of variation (%) | 2.28 | 30.9 | 50.7 |

Table 7 Measured Results of Strain at Break without Advanced Recycling Process (Average of N = 5)

| Strain rate (/s) | Yield stress (MPa) | Strain at break (%) | Break energy (J) |
|------------------------------|--------------------|---------------------|------------------|
| Average | 26.5 | 11.4 | 0.208 |
| Standard deviation | 0.669 | 2.71 | 0.0192 |
| Coefficient of variation (%) | 2.53 | 23.8 | 9.21 |
| Average | 23.9 | 16.2 | 0.273 |
| Standard deviation | 0.249 | 3.66 | 0.0786 |
| Coefficient of variation (%) | 1.04 | 22.5 | 28.8 |
| Average | 21.3 | 18.6 | 0.250 |
| Standard deviation | 0.767 | 4.64 | 0.0666 |
| Coefficient of variation (%) | 3.61 | 24.9 | 26.7 |

■ Hardness Evaluation

The hardness test was conducted using a dynamic ultra micro hardness tester (DUH-210). As the test pieces, ISO 527-2 1B test pieces were used. Fig. 7 shows the appearance of the instrument, and Table 8 shows the test conditions, which were set referring to ISO/TS 19278 (2019). Fig. 8 shows the test force-indentation depth curves with and without the advanced recycling process. Table 9 and Fig. 9 show the measured results of the indentation hardness (H_{IT}). The results with the advanced recycling process showed lower values of H_{IT} than those without the process. In Welch's t test of the results, a difference was seen at a significance level of 5 %.

Table 8 Test Conditions

| | |
|------------------------|--|
| Instrument | : DUH-210 |
| Indenter | : Berkovich indenter |
| Test mode | : Load/unload test |
| Test force | : 500 mN |
| Loading/unloading time | : 30 s |
| Load holding time | : 40 s |
| Number of tests | : 15 (central 10 tests were extracted) |
| Room temperature | : 23 ± 2 °C |
| Humidity | : 50 ± 10 % |



Fig. 7 DUH™-210

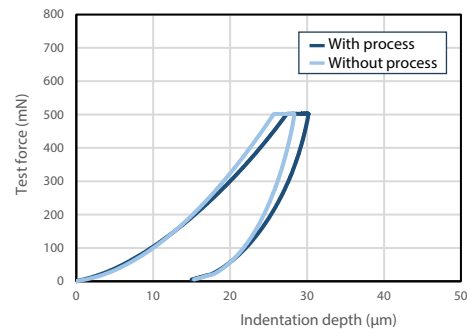


Fig. 8 Test Force-Indentation Depth Curves

Table 9 Measured Results of Indentation Hardness H_{IT} (N = 10)

| Test piece | Average (MPa) | Standard deviation | Coefficient of variation (%) |
|------------------------------------|---------------|--------------------|------------------------------|
| With advanced recycling process | 31.5 | 2.9 | 9.2 |
| Without advanced recycling process | 34.3 | 1.6 | 4.6 |

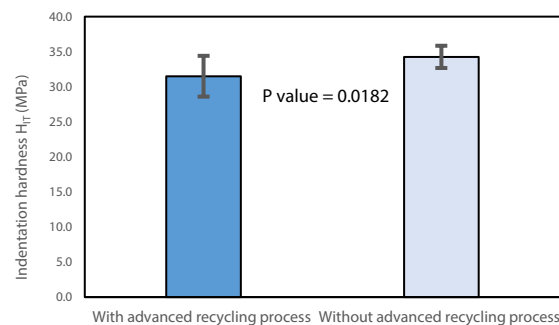



Fig. 9 Measured Results of Indentation Hardness H_{IT}

■ Evaluation of Crystallization Start Temperature by Thermal Analysis

This section presents the results of measurements with a differential scanning calorimeter (DSC), focusing on the crystallization start temperature in the cooling process after heating and melting the sample materials. The crystallization start temperature was measured 5 times each with the materials with and without the advanced recycling process. Fig. 10 shows the appearance of the instrument. Table 10 shows the measurement conditions, Fig. 11 shows representative DSC curves during cooling (blue line: with advanced recycling process, red line: without advanced recycling process), and Table 11 shows the measured results of the crystallization start temperature. The results confirmed that the crystallization start temperature with the advanced recycling process was lower than that without the process. Although not shown here, the heat of fusion in the heating process was also measured, and from the results, no significant difference could be seen in the degree of crystallization with and without the advanced recycling process.



| | |
|----------------------|--------------|
| Instrument | : DSC-60Plus |
| Heating/cooling rate | : 10 °C/min |
| Sample amount | : 6 mg |
| Atmosphere | : Nitrogen |

Fig. 10 DSC-60Plus

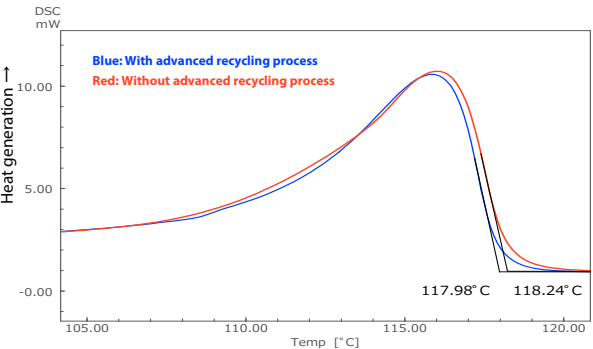


Fig. 11 DSC Curves for Crystallization (Cooling Process)

| Test material | Crystallization start temperature (°C) | |
|------------------------------------|--|--------------------|
| | Average | Standard deviation |
| With advanced recycling process | 117.93 | 0.064 |
| Without advanced recycling process | 118.26 | 0.080 |

Since differences in the mechanical properties and thermal properties could be seen in samples with and without the advanced recycling process, it is considered possible that the microscopic physical structures in the plastic were altered by the process. To evaluate this change from the microscopic viewpoint, we focused on the intermediate layers containing tie molecules, the crystal layer distribution, and the phase separation of PP in PE. The image of the tie molecules and intermediate layers is shown in Fig. 24.

■ Evaluation of Intermediate Layers, Including Tie Molecules, and Crystal Layer Distribution by SPM

The scanning probe microscope (SPM) is a microscope that scans a sample surface with a minute probe, enabling observation and measurement of the 3-dimensional shape of the sample and its local physical properties at high magnification. Fig. 12 shows the appearance of the instrument. Cross-sectional processing of the parallel part of the ISO 527-2 1B test pieces was done using a cryomicrotome, and the cross sections were measured under the observation conditions in Table 12. Fig. 13 and Fig. 14 show Topography images and elastic modulus images of the samples with and without the advanced recycling process, respectively.



Fig. 12 SPM-Nanoa™

| | |
|---------------------------|---|
| Instrument | : SPM-Nanoa |
| Scanner | : Medium-range scanner (XY: 30 μm, Z: 5 μm) |
| Observation mode | : Nano 3D Mapping™Fast |
| Observation field of view | : 300 nm × 300 nm, 100 nm × 100 nm, 30 nm × 30 nm |
| Pixel | : 256 × 256 |

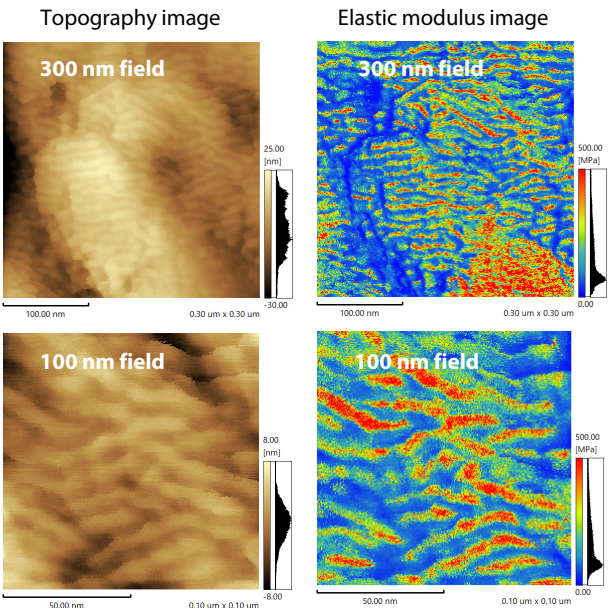


Fig. 13 Topography Images/Elastic Modulus Images with Advanced Recycling Process

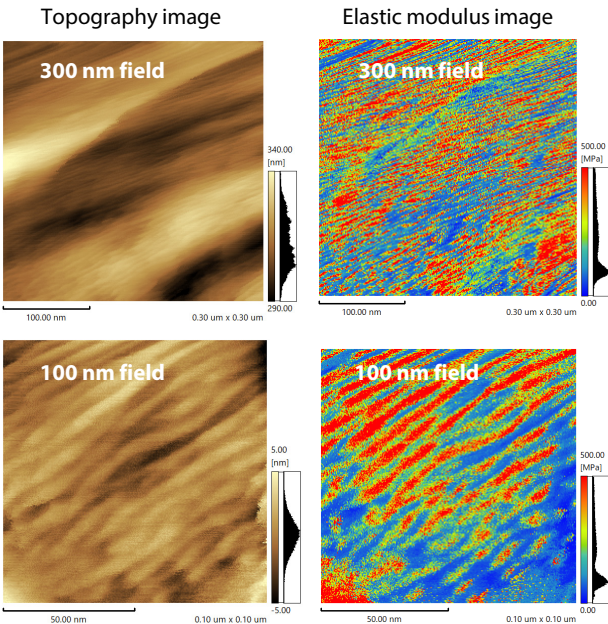


Fig. 14 Topography Images/Elastic Modulus Images without Advanced Recycling Process

Here, it can be understood that the microstructures in plastic can be grasped from the Topography images, and there were differences in the shapes of the lamellar crystals depending on whether the advanced recycling process was applied or not.

In the following, the intermediate layers, including tie molecules, are evaluated. In the elastic modulus images with the 100 nm field-of-view, the elastic modulus range from 0 to 500 MPa was divided into 100 MPa sections, and the area ratios in the observed field of view in each elastic modulus region were calculated by particle analysis software. Fig. 15 and Fig. 16 show the images of each elastic modulus region and their area ratios for the samples with and without the advanced recycling process, respectively. The white parts are areas with the elastic modulus indicated above each image. The 0 to 100 MPa region is considered to be an amorphous layer, while the 400 to 500 MPa region is considered to be a lamellar crystalline region. Since the elastic modulus of the band-shaped regions connecting pairs of lamellar crystals was 100 to 200 MPa, the 100 to 200 MPa region is thought to consist of intermediate layers that include tie molecules. Comparing the proportions of the intermediate layers by the area ratios in the 100 to 200 MPa region, the proportion of intermediate layers with advanced recycling process was 26.8 %, but was only 15.7 % without process, confirming that the area ratio of the intermediate layers is increased by the advanced recycling process. This region is considered to be the region which is responsible for the toughness and ductility of plastics.

Next, the crystal layer distribution is evaluated. If regions other than the amorphous layers and intermediate layers are considered to be crystalline layers, the regions from 200 to 500 MPa correspond to crystalline layers. In this case, no large difference was seen between the plastics with and without the advanced recycling process, as the respective area ratios were 26.8 % with the advanced recycling process and 26.1 % without the process. On the other hand, comparing the elastic modulus images of the 300 nm field of view in Figs. 13 and 14, there were differences in the length and distribution of the lamellar crystals. In comparison with the samples without the advanced recycling process, in the lamellar crystals with advanced recycling process, the longitudinal length of the crystals was short, the thickness of the crystals was large and the distance between the crystals was long. It is thought that the orientation of the lamellar crystals that were formed as a result of shearing in the molding process was moderated by the advanced recycling process. In order to evaluate the differences in the shapes of the lamellar crystals, a Fourier transform analysis of the elastic modulus images of the 300 nm field of view was carried out, focusing on the 400 to 500 MPa region, where lamellar crystals were observed. Fig. 17 shows the Fourier transform images with and without the advanced recycling process. The pattern of the bright spots is different with and without advanced recycling process. With process, a circular region exists near the center, but without process, a band-like region can be seen, and this region displays a periodic structure in the direction of the band. Based on this feature, it was judged that orientation of the lamellar crystals was higher in the samples without the advanced recycling process than in the samples with the process.

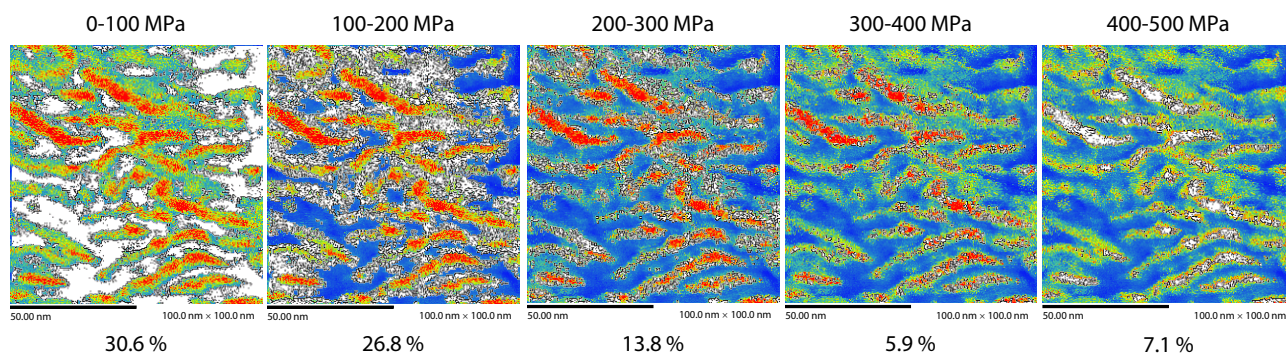


Fig. 15 Area Ratios of Elastic Modulus Regions of Sample with Advanced Recycling Process

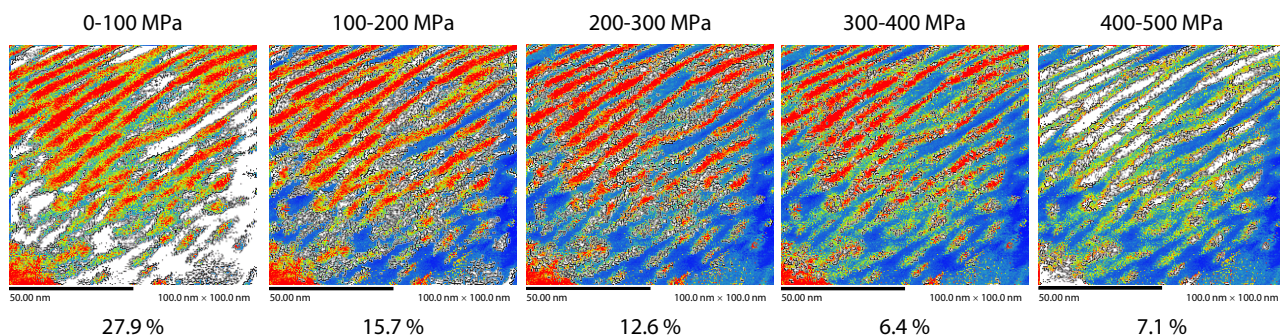


Fig. 16 Area Ratios of Elastic Modulus Regions of Sample without Advanced Recycling Process

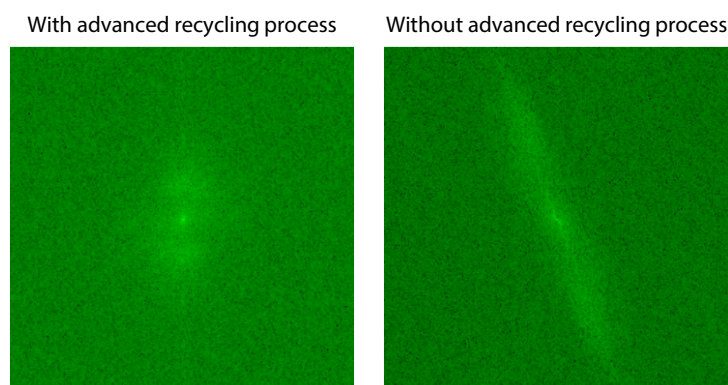


Fig. 17 Fourier Transform Images of Elastic Modulus Images of 300 nm Field of View

■ Evaluation of Phase Separation of PP in PE by FTIR

When evaluating recycled plastics, it is important to understand the materials that exist in the plastic. Various types of analytical instruments are used in component analysis of plastics, but among them, FTIR is widely used as an instrument that enables simple and easy analysis because complex sample preparation, such as dissolution of the sample in a solvent, is not necessary.

Here, in order to evaluate the areal distribution of the components, sample slices with a thickness of 15 μm were prepared using a microtome, and area mapping measurements were carried out by the transmission method using the infrared mode of the AIRsight infrared and Raman microscope. Fig. 18 shows the appearance of the instruments. In these measurements, the instrument was set to an aperture of 50 $\mu\text{m} \times 50 \mu\text{m}$, and the mapping range of 450 $\mu\text{m} \times 450 \mu\text{m}$ was measured in 50 μm steps. This enables uninterrupted measurement of the entire measurement range set for the experiment. Table 13 and Fig. 19 show the measurement conditions and an observation image of the measurement range, respectively.



Fig. 18 IRXross™ and AIRsight™

Table 13 Measurement Conditions

| | |
|----------------------|--|
| Instrument | : IRXross™, AIRsight (infrared mode) |
| Resolution | : 8 cm^{-1} |
| Accumulation | : 50 times |
| Apodization function | : Happ-Genzel |
| Aperture size | : 50 $\mu\text{m} \times 50 \mu\text{m}$ |
| Step width | : 50 μm |
| Mapping range | : 450 $\mu\text{m} \times 450 \mu\text{m}$ |
| Detector | : T2SL |

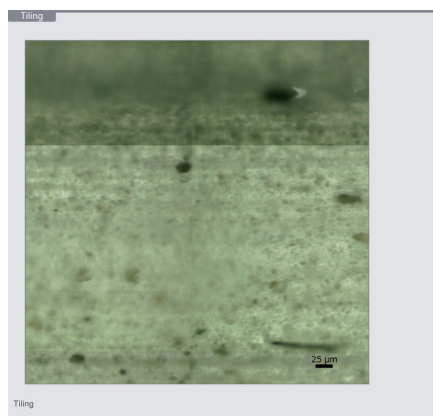


Fig. 19 Observation Image of Measurement Range (without process)

Fig. 20 shows representative infrared spectra obtained from samples both with and without the advanced recycling process. No large differences were observed in the infrared spectra with and without process.

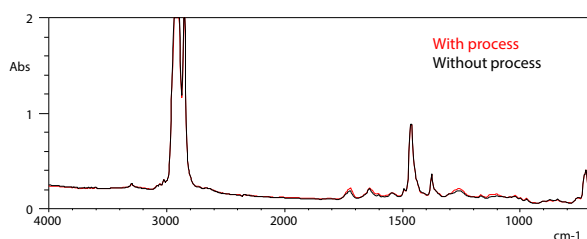


Fig. 20 Representative Infrared Spectra Obtained from Samples with/without Advanced Recycling Process

Next, Fig. 21 shows the results of a library search, which revealed that the component detected by FTIR is a PE-rich recycled plastic. On the other hand, from an examination of the enlarged view of the low frequency region, where the peaks were not saturated, it is estimated that the plastic also contains polypropylene (PP) (green arrow).

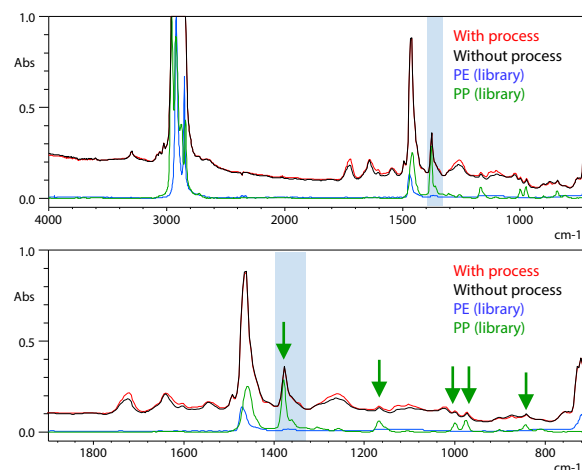


Fig. 21 Search Results of Infrared Spectrum of Specimen with Advanced Recycling Process (Top: Full Spectrum, Bottom: Enlarged View of Low Frequency Region)

Segregation of individual components such as PP is thought to become a point of origin for cracking, making the material more prone to break. Therefore, in this study, a chemical image was prepared by the peak height of 1378 cm^{-1} (CH_3 symmetric deformation vibration), which is considered to originate from PP. The analysis conducted $n = 6$ times. Among the data, Fig. 22 and Fig. 23 show the representative chemical images. The images become increasingly red as the peak height increases.

In comparison with the sample without the advanced recycling process, the sample with the process displays numerous yellow areas, indicating that segregation of PP is slight. However, without the process, localized red areas can be observed, suggesting segregation of PP. Based on these results, it was found that segregation of component substances in recycled plastic material is eliminated by the advanced recycling process. Moreover, as demonstrated by this experiment, it was also possible to visualize the improvement of the physical properties of recycled plastic achieved by the advanced recycling process.

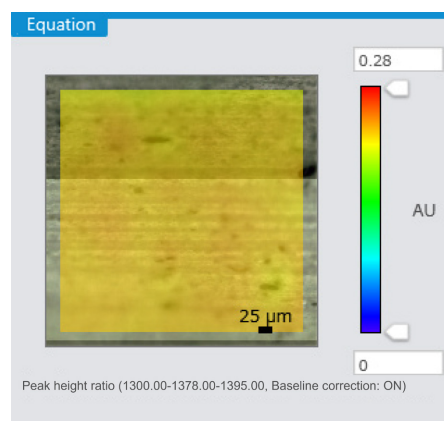


Fig. 22 Chemical Image of PP Component Distribution in Plastic with Advanced Recycling Process

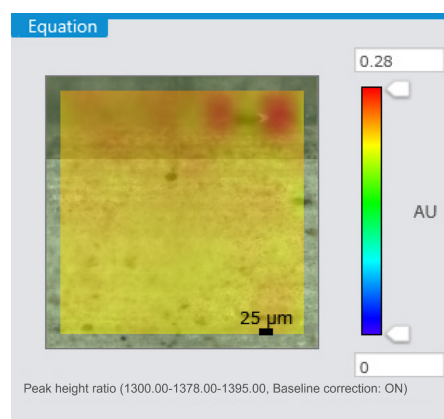


Fig. 23 Chemical Image of PP Component Distribution in Plastic without Advanced Recycling Process

■ Relationship of Strain at Break, Impact Property, and Microscopic Physical Structure

The distribution of the elastic modulus obtained by SPM revealed that the advanced recycling process increases the proportion of intermediate layers containing tie molecules. Since this region is responsible for the toughness and ductility of plastics, it is thought that this change in the microscopic physical structure results in improvement of strain at break and the impact property. Because the FTIR results indicated that aggregation of PP is slight when advanced recycling process is applied, the PE content has a continuous distribution, and as a result, it displays superior resistance to break. Without the process, aggregation of PP is large, and if loading cause deformation, break can be expected to occur easily, with an area having a high concentration of PP as the point of origin. Summarizing this discussion, it is suggested that the higher continuity of the PE obtained by the advanced recycling process contributes to the improved strain at break and impact property of recycled plastic with this process. Thus, strain at break and impact property are improved by two factors: an increase in the region containing tie molecules, as mentioned above, and the improved continuity of the PE distribution.

■ Study of Changes in Microscopic Physical Structure Based on Combination of Individual Evaluation Results

The elastic modulus and H_{IT} decreased as a result of the advanced recycling process. Because the elastic modulus and H_{IT} are low when the degree of crystallization is low, and intermediate layers containing tie molecules are responsible for viscosity and ductility, it can be thought that an increase in the intermediate layers containing tie molecules will lead to a decrease in the elastic modulus and H_{IT} . However, if the discussion is limited to only the elastic modulus and H_{IT} , it is not possible to judge whether the decrease in the elastic modulus and H_{IT} is due to the decrease in the degree of crystallization or the increase in intermediate layers containing tie molecules. Therefore, in proceeding with this study, the DSC results were also used. In the evaluation of the heat of fusion by DSC, no difference in the degree of crystallization could be detected. Since the elastic modulus and H_{IT} decreased even though there was no large difference in the degree of crystallization, the cause of this decrease can be attributed to the increase in the intermediate layers containing tie molecules. Similarly, in the results of the elastic modulus distribution by SPM, there was no significant difference in the area ratio of the crystalline layer, but the area ratio of the intermediate layers containing tie molecules increased as a result of the advanced recycling process. The discussion based on the elastic modulus, H_{IT} , and the heat of fusion is also consistent with the results of the elastic modulus distribution obtained by SPM. Thus, it is considered possible to evaluate changes in the intermediate layers containing tie molecules by using a combination of simple evaluation techniques, namely, the elastic modulus, H_{IT} , and the heat of fusion.

Next, the crystallization start temperature in the DSC results decreased with the advanced recycling process. This is attributed to a delay in crystallization because the motion of molecule chains is suppressed by an increase in polymer entanglements due to the heat treatment applied in the advanced recycling process. It is also thought that the increase in polymer entanglements in the molten condition brings about an increase in intermediate layers containing tie molecules accompanying crystallization.

Based on the above discussion, it is suggested that an evaluation approach utilizing a combination of the elastic modulus, H_{IT} , the heat of fusion, and the crystallization start temperature is effective as a simple evaluation technique for understanding the changes in the microscopic physical structure with high sensitivity. The validity of this evaluation technique could also be verified by the evaluation of the elastic modulus distribution by SPM.

Evaluations of changes in the microscopic physical structure of plastics generally require an evaluation using large-scale instruments such as X-ray small angle scattering, synchrotron X-ray, and the transmission electron microscope (TEM). However, as demonstrated in this example, the microscopic physical structure of plastics can be estimated by using a combination of general-purpose evaluation techniques.

■ Effectiveness and Distinctive Features of Individual Evaluation Methods

Since it is possible to acquire stress-strain curves under high speed conditions by the high speed tensile test, the stress-strain curves required in simulations of collision impact and dropping can be obtained. Thus, it is possible to evaluate safety-related material properties in the stage of studying recycled plastics for adoption in products.

The hardness test is a highly sensitive evaluation technique for understanding changes in the microscopic physical structure. Since evaluation is possible by simply preparing sheet-form samples, the results can be used as an index to predict the properties of the materials to be used in the pre-production stage.

Thermal analysis to evaluate the crystallization start temperature is also an effective evaluation technique for estimating differences in polymer entanglements. Because sample preparation is also comparatively simple, and it is not necessary to select the sample shape, this is an effective technique for evaluations of the degree of crystallization and thermal properties of materials in each stage of the production process.

Infrared and Raman spectroscopy makes it possible to visualize the phase separation structure in the micron region, and is effective for understanding the causes of changes in physical properties due to the material selection, blend, and adjustment of the manufacturing conditions. Although not discussed in this report, the AIRSight microscope enables evaluation by Raman spectroscopy on the same axis as infrared spectroscopy, supporting simultaneous multifaceted evaluation.

SPM is an evaluation technique that makes it possible to visualize the physical structure in the sub-micron region, providing a direct grasp of changes in the microscopic physical structure. It is effective for understanding the causes of changes in physical properties due to the material selection, blend, and adjustment of the manufacturing conditions.

■ Conclusion

This study demonstrated that strain at break and the impact property are improved by the newly-developed advanced recycling process. It was suggested that this improvement in strain at break and the impact property is the result of two factors: an increase in the intermediate layers containing tie molecules, and improvement of the continuity of the distribution of PE.

Use of a combination of evaluations of the elastic modulus, the indentation hardness H_{IT} , the heat of fusion, and the crystallization start temperature is considered to be effective as simple evaluation technique for understanding changes in the microscopic physical structure with high sensitivity.

■ Reference: Image of Entanglements during Melting of Polymers and Crystal Structure after Cooling²⁾

As reference, the following diagram shows the image of the aggregation state of polymers explained in the main text. If entanglements of the molecules are increased by heat treatment in the advanced recycling process, the number of tie molecules after crystallization will increase.

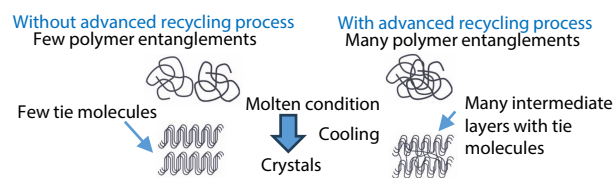


Fig. 24 Image of Aggregation State of Polymers

<References>

- 1) Shigeru Yao and Aya Tominaga: Novel Technology Development on Plastic Material Recycling, Haikibutsu Shigen Junkan Gakkaishi, 29, 2, pp. 116-124, 2018
- 2) Present and future of waste plastics: plastic resource circulation in sustainable society, The Japan Institute of Energy, p. 147

DUH, AGX, TRAPEZIUM, HITS, IRXross, AIRSight, SPM-Nanoa, and Nano 3D Mapping are trademarks of Shimadzu Corporation or its affiliated companies in Japan and/or other countries.



SHIMADZU

Shimadzu Corporation

www.shimadzu.com/an/

For Research Use Only. Not for use in diagnostic procedures.

This publication may contain references to products that are not available in your country. Please contact us to check the availability of these products in your country.

The content of this publication shall not be reproduced, altered or sold for any commercial purpose without the written approval of Shimadzu. See <http://www.shimadzu.com/about/trademarks/index.html> for details.

Third party trademarks and trade names may be used in this publication to refer to either the entities or their products/services, whether or not they are used with trademark symbol "TM" or "®".

Shimadzu disclaims any proprietary interest in trademarks and trade names other than its own.

The information contained herein is provided to you "as is" without warranty of any kind including without limitation warranties as to its accuracy or completeness. Shimadzu does not assume any responsibility or liability for any damage, whether direct or indirect, relating to the use of this publication. This publication is based upon the information available to Shimadzu on or before the date of publication, and subject to change without notice.

01-00867-EN

First Edition: Jul. 2025

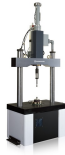
➤ Please fill out the survey

Related Products

Some products may be updated to newer models.



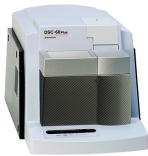
➤ **AUTOGRAPH AGX-V2 Series**
Precision Universal Testing Machines



➤ **HITS-X Series**
High-Speed Impact Testing Machines



➤ **DUH-211/DUH-211S**
Dynamic Ultra Micro Hardness Tester



➤ **DSC-60 Plus Series**
Differential Scanning Calorimeter



➤ **AIRsight**



➤ **SPM-Nanoa**
Scanning Probe Microscope/Atomic Force Microscope

Related Solutions

➤ Chemicals

➤ Plastics

➤ Price Inquiry

➤ Product Inquiry

➤ Technical Service /
Support Inquiry

➤ Other Inquiry